Delayed Positive Thallium Uptake in Large B-Cell Non-Hodgkin's Malignant Lymphoma

Hussein M. Abdel-Dayem, Sleiman Y. Naddaf, Walid S. Omar, Mohamed Aziz and John Gillooley
Nuclear Medicine Section, Department of Radiology and Department of Pathology, Saint Vincent's Hospital and Medical Center of New York and New York Medical College, Valhalla, New York

We report an unusual finding in an AIDS patient who presented with a large mediastinal mass and multiple lymphadenopathy. A sequential thallium and gallium scan to specify the nature of the mediastinal mass was requested. The early thallium images, acquired 15 min after the intravenous injection, showed no uptake in the mass. The delayed images 2 hr later showed intense thallium uptake. A gallium scan perfomed 48 hr later also showed intense gallium uptake in the mediastinal mass. Biopsy from the inguinal lymph node confirmed the presence of large-cell diffuse noncleaved malignant lymphoma. This case raises questions about the optimum time of imaging for thallium in high-grade lymphoma, whether delayed imaging is essential, about previous reports of low sensitivity of thallium in undifferentiated lymphoma and about the mechanism of thallium uptake in this type of tumor.

Key Words: thallium-201-chloride; undifferentiated lymphoma; AIDS

J Nucl Med 1997; 38:1213–1215

Thallium-201-chloride is used for tumor imaging to differentiate benign from malignant lesions and for the follow-up of patients treated for malignant disease (*1–5*). Sites of the most common clinical applications include the brain, bones (*6–11*) and soft tissues (*12–14*). The mechanism of uptake of thallium in malignant tumors has been reported to be related to blood flow, ATPase and sodium pump activity and indirectly related to glucose and energy utilization (*15–17*). The optimum time for thallium imaging has been reported to be between 10–20 min after the intravenous injection (*18*). We are reporting an unusual case of high-grade malignant lymphoma in an AIDS patient in whom the early thallium images started acquisition 15 min after the intravenous injection of thallium showed no uptake in the mediastinal mass. The delayed images acquired 2 hr later showed intense uptake of thallium. A subsequent gallium scan 48 hr later showed intense gallium uptake at the same location. The unusual findings of this case are contrary to what have been related previously in the literature. This raises several questions that are discussed.

CASE REPORT

A 47-yr-old HIV-positive man with AIDS was admitted on July 18, 1996 because of the presence of inguinal lymph nodes. A chest radiograph at admission revealed a large mediastinal mass (Fig. 1). Laboratory tests showed RBC 0.6 × 10^6/MCL, hemoglobin 8.7 g/dl, CD4 70. WBC showed a total of 2800/MCL with lymphocytes 17%, neutrophils 75%, platelets 156 × 10^3/MCL, LDH was increased at 3317 IU/liter, total bilirubin 1.1 mg/dl, alkaline phosphatase 95 IU/liter and AST 79 IU/liter, and serum hepatitis studies were negative. A bone marrow biopsy was negative for lymphoma. CSF cytology revealed an atypical population of large

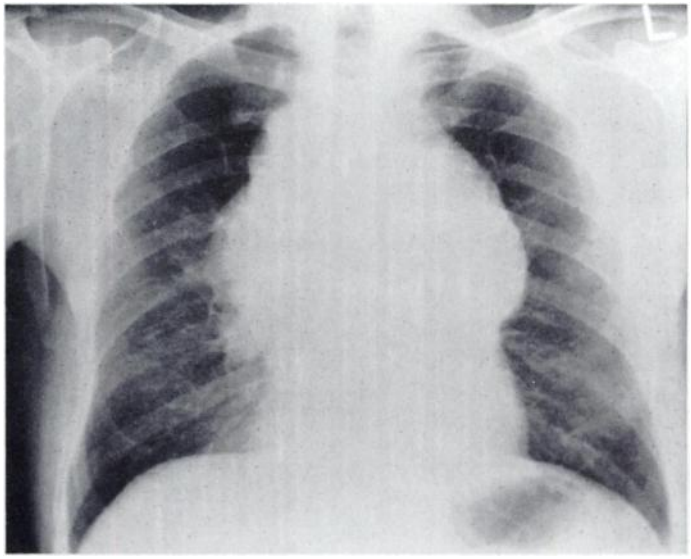

FIGURE 1. Chest radiograph at time of admission showing large mediastinal mass.

lymphoid cells suspicious for malignant lymphoma. CT of the abdomen on July 19, 1996 showed enlarged lymph nodes in the retroperitoneal region and the gastro-hepatic ligament. The thallium study was performed on July 23, 1996. Fifteen minutes after the intravenous injection of 4.0 mCi (148 MBq) planar images of the chest in the anterior and posterior projection showed no evidence of increased uptake in the mediastinum (Fig. 2, upper row). The delayed planar images acquired 2 hr later showed intense uptake in the mediastinal mass and in the left supraclavicular region (Fig. 2, lower row). A dose of 8 mCi (288 MBq) of ^{67}Ga-citrate was injected intravenously. Forty-eight hours later, total-body planar images showed intense gallium uptake in the mediastinal mass with focal uptake in the left supraclavicular region and in the upper abdomen most likely in the gastro-hepatic region or in the left lobe of the liver (Fig. 3). An excisional biopsy from the inguinal lymph node revealed total effacement of the lymph node due to an infiltrate of large malignant lymphoid cells with numerous mitotic figures (Fig. 4). The diagnosis of non-Hodgkin's high-grade malignant lymphoma (according to the revised European American Lymphoma Classification "REAL"), large B-cell type, diffuse was confirmed by immunohistochemical studies.

DISCUSSION

Thallium-201-chloride has been widely used for tumor imaging (*1*). A previous report suggested that its sensitivity in high-grade malignant lymphoma is lower than in the low-grade types (*19*). Gallium-67-citrate on the other hand, has been reported to be more sensitive in high-grade lymphoma than in the low-grade types (*19*). Recently, sequential thallium and gallium scans have been reported by us and others to be useful in AIDS patients in differentiating Kaposi's sarcoma from

Received Sep. 4, 1996; revision accepted Dec. 10, 1996.
For correspondence or reprints contact: Hussein M. Abdel-Dayem, MD, Director of Nuclear Medicine Section, Department of Radiology, St. Vincent's Hospital and Medical Center, 153 W. 11th St., New York, NY 10011.

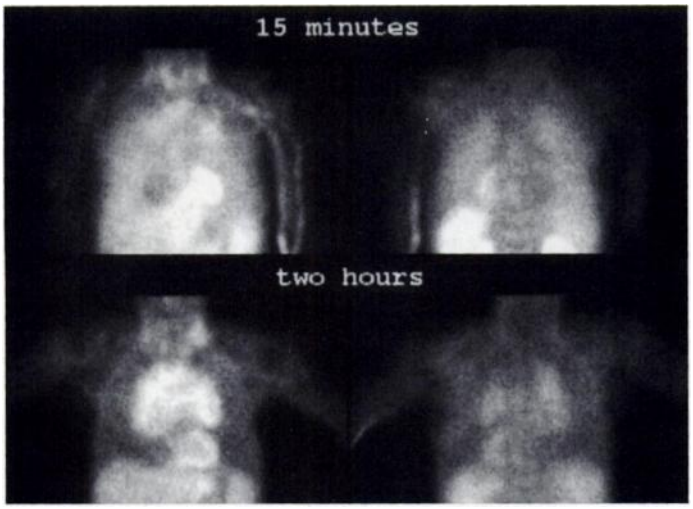

FIGURE 2. Early and delayed thallium images acquired 15 min (upper row) and 2 hr later (lower row) showing no thallium uptake in the mediastinal mass at the 15-min images and marked increased uptake in the 2-hr images.

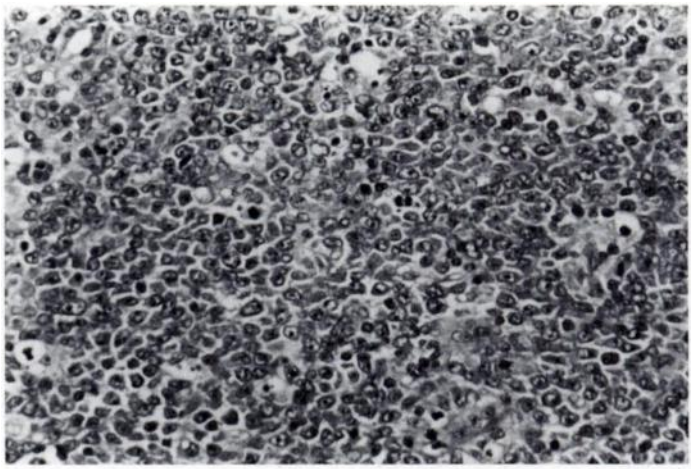

FIGURE 4. Pathological slide of specimen from excised inguinal lymph node. High-power view of the inguinal lymph node showing large malignant lymphoid cells with mitotic figures.

malignant lymphomas or acute inflammatory conditions (*20–22*). Lesions that are positive for both thallium and gallium are suggestive of malignant lymphoma. Malignant lymphoma in AIDS patients is characterized by an aggressive course, undifferentiated pathology similar to Burkitt's-type lymphoma and by involvement of extranodal sites such as brain, heart, stomach and small bowel. In order to differentiate between inflammatory and malignant lymphomas or Kaposi's sarcoma, early and delayed thallium images were proposed. In benign or inflammatory lesions, early thallium uptake usually clears with time while in malignant lymphoma or Kaposi's sarcoma, thallium uptake persists in the delayed images with minimal changes (*23,24*).

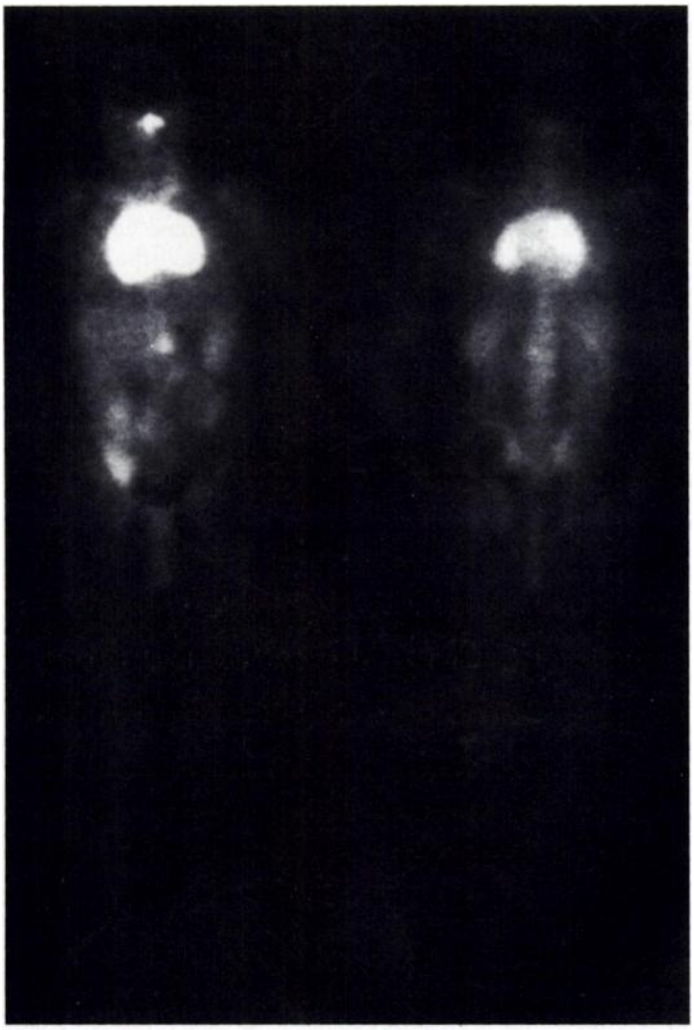

FIGURE 3. Total-body gallium images acquired 48 hr following the intravenous injection of 8 mCi (288 MBq) ^{67}Ga-citrate showed intense uptake in the mediastinal mass, left supraclavicular region and upper abdomen.

The optimum time for thallium imaging in tumors has been previously reported between 10–20 min after the intravenous injection (*18*). There are no previous reports of a negative thallium uptake in malignant tumors in the early images that became highly intense in the delayed images similar to the one we are presenting in this manuscript. The discrepancy in this case raises three questions: What is the optimum time of imaging? What is the accuracy of the previously reported low sensitivity of thallium in high-grade malignant lymphoma? What is the mechanism of thallium uptake? In all the previous reports, the thallium studies were evaluated only by early images within 30 min after the intravenous injection. Chen, in his presentation about optimum time for thallium imaging in patients with lymphoma, reported that delayed imaging was more sensitive than early imaging (*25*). The sensitivity of the thallium in high-grade lymphoma might increase if delayed images were obtained. Our own experience is similar to what is reported in the literature of the poor sensitivity for thallium in AIDS patients with malignant lymphoma. We obtain early images in all patients and perform delayed images only if there were abnormal sites of thallium uptake in the early images. The presence of a large mediastinal mass in the case presented here raised our doubts and we decided to obtain the delayed images. We have changed our protocol to acquire both early and delayed thallium images whenever there is a high clinical suspicion of malignancy or in the presence of a mediastinal mass.

We conclude from this case that the mechanism of thallium uptake in high-grade undifferentiated lymphoma is not fully understood. Causes of false-negative thallium uptake could be related to tumor necrosis. Our intention by the early reporting of this case is to draw the attention of nuclear medicine physicians involved with thallium in tumor imaging to the drawback of relying only on early images. Delayed images might be essential to increase the sensitivity of tumor detection. More work is needed in thallium tumor imaging.

REFERENCES

1. Abdel-Dayem HM, Scott AM, Macapinlac HA, El-Gazzar AH, Larson SM. Role of Tl-201 chloride and Tc-99m-sestamibi in tumor imaging. In: Freeman LM, ed. *Nuclear Medicine Annual* New York, NY: Raven Press; 1994:181–234.
2. El-Gazzar AH, Fernandez-Ulloa M, Silberstein EG. Thallium-201 as a tumor imaging agent: current status and future consideration. *Nucl Med Commun* 1993;14:96–99.
3. El-Gazzar AH, Malki A, Abdel-Dayem HM, et al. Role of Tl-201 in the diagnosis of solitary bone lesions. *Nucl Med Commun* 1989:477–485.
4. Waxman A, Ramanna L, Memsie L, Silberman A, Brennar J. Thallium scintigraphy in the differentiation of malignant from benign mass abnormalities of the breast [Abstract]. *J Nucl Med* 1990;31:767.
5. Waxman AD, Ramannah L, Memsie LD, et al. Thallium scintigraphy in the evaluation of mass abnormalities of the breast. *J Nucl Med* 1993;34:18–23.
6. Ramannah L, Waxman AD, Weiss A, Rosen G. Thallium-201 scan patterns in bone and soft tissue sarcoma [Abstract]. *J Nucl Med* 1992;33:843.
7. Kim KT, Black KL, Marcino D, et al. Thallium-201 SPECT imaging of brain tumors; methods and results. *J Nucl Med* 1990;19:965–969.
8. Kaplan WD, Takuovian T, Morris J, et al. Thallium-201 brain tumor imaging: a comparative study with pathologic correlation. *J Nucl Med* 1987;28:47–52.
9. Gruber MC, Hochberg FH. Editorial: systemic evalution of primary brain tumors. *J Nucl Med* 1990;31:969–971.
10. Sjoholm BA, Elmquist D, Rehncrona S, Rosen I, Salford L. Thallium-201 and SPECT distinguishes high-grade from low-grade gliomas [Abstract]. *J Nucl Med* 1992;33:868.
11. Kosuda S, Aoki S, Suzuki K, Nakamura O, Shidara N. Reevaluation of quantitative thallium-201 brain SPECT for brain tumors [Abstract]. *J Nucl Med* 1992;33:844.
12. Hoh CK, Khannas S, Harris GC, et al. Evaluation of brain tumor recurrence with Tl-201 SPECT studies: correlation with FDG PET and histological results [Abstract]. *J Nucl Med* 1992;33:867.
13. Ramannah L, Waxman AD, Binney G, Waxman S, Mirra J, Rosen G. Tl-201 scintigraphy in bone sarcoma: comparison with Ga-67 and Tc-99m-MDP in the evaluation of chemotherapeutic response. *J Nucl Med* 1990;31:567–571.
14. Caluser C, Macapinlac H, Meyers P, et al. The relationship between thallium uptake, blood flow and blood pool radioactivity in bone and soft tissue tumors. *Clin Nucl Med* 1992;17:565–571.
15. Kostakoglu L, David PM, Divgi CR, Botet J, Healy J, Larson SM. Correlation of the findings of thallium-201 chloride scans with those of other imaging modalities and histology following therapy in patients with bone and soft tissue sarcomas. *Eur J Nucl Med.* 1995;22:1232–1237.
16. Sehweil AM, Mckillop JH, Milroy R, et al. Mechanism of Tl-201 uptake in tumors. *Eur J Nucl Med* 1989;15:376–379.
17. Ando A, Ando I, Katayana M, et al. Biodistribution of Tl-201 in tumor bearing animals and inflammatory lesions induced animals. *Eur J Nucl Med* 1987;12:567–572.
18. Sehweil A, McKillop JH, Ziada G, Al-Sayed M, Abdel-Dayem HM, Omar YT. The optimum time for tumor imaging with thallium-201. *Eur J Nucl Med* 1988;13:527–529.
19. Kaplan WD, Southee ML, Annese MS, et al. Evaluating low and intermediate grade non-Hodgkin's lymphoma (NHL) with gallium-67 and thallium-201 imaging [Abstract]. *J Nucl Med* 1990;31:793.
20. Abdel-Dayem HM, DiFabrizio L, Bag R, Aras T, Turoglu HT, Kempf JS, Habbab N, Pescatore F, Sadik A, Kowalsky W. Evaluation of sequential thallium and gallium scans in AIDS patients. *J Nucl Med* 1996;37:1662–1667.
21. Abdel-Dayem HM, DiFabrizio L, Aras T, et al. Prospective evaluation of sequential thallium-201 chloride and gallium-67 citrate scans in AIDS patients [Abstract]. *J Nucl Med* 1993;34:172P.
22. Lee VW. AIDS-related Kaposi's sarcoma–findings in thallium-201 scintigraphy. *Am J Roentgenol* 1988;151:1233–1235.
23. Ganz WI, Nguyen TQ, Benedetto MP, et al. Use of early, late and SPECT thallium imaging in evaluating activity of soft tissue and bone tumors [Abstract]. *J Nucl Med* 1993;34:32P.
24. Ueda T, Kaszi Y, Yakisaka S, et al. Time sequential single-photon emission computed tomography studies in brain tumor using thallium-201. *Eur J Nucl Med* 1993;20:138.
25. Chen DCP, Ma GQ, Ansari A, et al. Optimal imaging time for thallium as a tumor agent in patients with lymphoma [Abstract]. *J Nucl Med* 1992;33(suppl):44P.

PET 2-Fluoro-2-Deoxyglucose Uptake in Rat Prostate Adenocarcinoma During Chemotherapy with Gemcitabine

Uwe Haberkorn, Matthias E. Bellemann, Annette Altmann, Ludwig Gerlach, Iris Morr, Franz Oberdorfer, Gunnar Brix, Josef Doll, Johannes Blatter and Gerhard van Kaick

Department of Oncological Diagnostics and Therapy, German Cancer Research Center, Heidelberg, Germany; and Lilly Deutschland, Bad Homburg, Germany

This study was performed to investigate the effect of the new chemotherapeutic agent gemcitabine on glucose transport and metabolism in prostate carcinoma in vitro and in vivo. **Methods:** After transplantation of rat prostate adenocarcinoma cells, dynamic PET measurements with fluorine-18-labeled 2-fluoro-2-deoxy-D-glucose (^{18}FDG) were performed in 15 animals before and 1 day after therapy with 90 mg/kg of body weight (n = 8) and 180 mg/kg of body weight (n = 7) gemcitabine. In the second examination, the animals received a simultaneous injection of ^{18}FDG and [^{3}H]thymidine. Quantitative evaluation of the PET data was done using the standardized uptake value (SUV) as well as a three-compartment pharmacokinetic model. Furthermore, the incorporation of [^{3}H]thymidine into the DNA was determined. In vitro measurements of the FDG, 3-O-methylglucose and thymidine uptake were performed immediately and 4 hr after a 24-hr incubation period with different doses of gemcitabine. **Results:** FDG–SUV and the metabolic rate of FDG utilization did not change significantly after therapy. However, the values for the transport rate constants K_1 and k_2 increased significantly. The incorporation of thymidine into the DNA of treated tumors showed an 80% decline as compared with a control group. In the cell culture experiments, a dose-dependent increase of FDG (up to 178%) and 3-O-methylglucose uptake (up to 305%) was demonstrated. The thymidine uptake showed a 96% decline in the nucleic acid fraction and an increase of up to 337% in the cytoplasmic fraction. **Conclusion:** The more global measures of FDG metabolism as SUV and metabolic rate of FDG utilization were unchanged after therapy, while DNA synthesis and cell viability declined. However, in vitro and in vivo evidence of an enhancement of glucose transport is presented, indicating that quantification by modeling may be superior for the evaluation of metabolic effects during chemotherapy.

Key Words: fluorine-18-FDG; PET; gemcitabine; prostate adenocarcinoma; chemotherapy

J Nucl Med 1997; 38:1215–1221

Gemcitabine (2′,2′-difluoro-2′-deoxycytidine, dFdC) is a novel anticancer agent that must be metabolized in the cell into its active nucleotide forms. The drug is phosphorylized by deoxycytidine kinase, which is the rate-limiting enzyme for the formation of the active anticancer metabolites: dFdC diphosphate and dFdC triphosphate. dFdC diphosphate inhibits ribonucleotide reductase (*1*), the enzyme that produces deoxynucleotides required for DNA synthesis and repair. Subsequently, deoxycytidine triphosphate (dCTP) levels decrease, which is important because dFdC triphosphate competes with dCTP for incorporation into DNA by DNA polymerases (*2*). The decrease of the cellular concentration of dCTP results in an increase of the gemcitabine incorporation into the DNA, a self-potentiating mechanism. After the gemcitabine nucleotide is incorporated at the end of the elongating DNA strand, one more nucleotide is

Received Aug. 1, 1996; revision accepted Nov. 6, 1996.

For correspondence or reprints contact: Uwe Haberkorn, MD, Department of Oncological Diagnostics and Therapy, German Cancer Research Center, Im Neuenheimer Feld 280, D-69120 Heidelberg, Germany.